

*Eigenstate-Specific Temperatures in Two-Level Paramagnetic Spin Lattices*

Mark B. Masthay, Calley N. Eads, Amber N. Johnson, Robert G. Keil, Philip Miller,

Ross E. Jones, Joe D. Mashburn, and Harry B. Fannin

**APPENDIX A:** Spin Permutation Antisymmetries of the ESTs in PSLs.....p. 2

**APPENDIX B:** System Size-Dependence of Constant- $X_j$ , Decreasing- $X_j$ , and Increasing- $X_j$   
Eigenstates in Two-Level PSLs..... p. 7

**REFERENCES:** .....p. 12

## APPENDIX A

### SPIN PERMUTATION ANTISYMMETRIES OF THE ESTs IN PSLs

Permuting the number of spin-up and spin-down lattice sites is graphically equivalent to moving from the lower (positive temperature) branches to the upper (negative temperature) branches of the microcanonical and canonical energy vs. entropy profiles,  $T_c^{conv}$  and the four ESTs thus change sign upon permuting  $N_\uparrow$  and  $N_\downarrow$ —and consequently manifest *spin permutation antisymmetries*—as detailed below.<sup>1-3</sup>

#### 1. Spin Permutation Antisymmetries of the Continuous ESTs

The continuous ESTs change sign upon permuting  $N_\uparrow = N - j$  and  $N_\downarrow = j$  provided  $j \neq N/2$ ; *i.e.*, they manifest the spin permutation antisymmetries

$$T_\mu^{N-j \rightarrow N-j+1} = \frac{\varepsilon}{k(\Psi_0[j+1] - \Psi_0[N-j+1])} = -\frac{\varepsilon}{k(\Psi_0[N-j+1] - \Psi_0[j+1])} = -T_\mu^{j \rightarrow j+1} \quad (\text{A1a})$$

and

$$T_c^{N-j \rightarrow N-j+1} = \frac{\varepsilon}{k \ln\left(\frac{j}{N-j}\right)} = -\frac{\varepsilon}{k \ln\left(\frac{N-j}{j}\right)} = -T_c^{j \rightarrow j+1}, \quad (\text{A1b})$$

in accordance with Eqs. (8a,10), Figs. A-1,A-2, and Table I. Hence, the tangential slopes at the initial eigenstates of the negative temperature  $[j, N-j] \rightarrow [j-1, N-j+1]$  transitions on the upper branches of the profiles are equal in magnitude but opposite in sign to the slopes at the initial eigenstates of the positive temperature  $[N-j, j] \rightarrow [N-j-1, j+1]$  transitions directly below them on the lower branches (*e.g.*,  $T_\mu^{8 \rightarrow 9} = -T_\mu^{2 \rightarrow 3}$  and  $T_c^{8 \rightarrow 9} = -T_c^{2 \rightarrow 3}$ ).<sup>4</sup>

## 2. Spin Permutation Antisymmetries of the Discrete ESTs

The discrete ESTs manifest the spin permutation antisymmetries

$$T_{d\mu}^{N-j-1 \rightarrow N-j} = \frac{\varepsilon}{k \ln \left( \frac{j+1}{N-j} \right)} = - \frac{\varepsilon}{k \ln \left( \frac{N-j}{j+1} \right)} = - T_{d\mu}^{j \rightarrow j+1} \quad (\text{A2a})$$

and

$$T_{dc}^{N-j-1 \rightarrow N-j} = \frac{\varepsilon}{k \ln \left[ \frac{(N-j-1)^{(N-j-1)} (j+1)^{(j+1)}}{(N-j)^{(N-j)} j^j} \right]} = - \frac{\varepsilon}{k \ln \left[ \frac{(N-j)^{(N-j)} j^j}{(N-j-1)^{(N-j-1)} (j+1)^{(j+1)}} \right]} = - T_{dc}^{j \rightarrow j+1}, \quad (\text{A2b})$$

in accord with Eqs. (12,13). The discrete slopes between the initial and final eigenstates of  $\Delta j = +1$  negative temperature  $[j+1, N-j-1] \rightarrow [j, N-j]$  transitions on the upper branches of the energy *vs.* entropy profiles are thus equal in magnitude but opposite in sign to those between the initial and final eigenstates of  $\Delta j = +1$  positive temperature  $[N-j, j] \rightarrow [N-j-1, j+1]$  transitions on the lower branches provided  $j \neq N$ . Hence, the final eigenstates  $[j, N-j]$  of the negative temperature transitions lie directly above the initial eigenstates  $[N-j, j]$  of the positive temperature transitions (*e.g.*,  $T_{d\mu}^{7 \rightarrow 8} = -T_{d\mu}^{2 \rightarrow 3}$  and  $T_{dc}^{7 \rightarrow 8} = -T_{dc}^{2 \rightarrow 3}$ ), as detailed in Figs. 2,A-1,A-2 and Table I. Notably, the spin permutation antisymmetries of the discrete ESTs differ from those of the continuous ESTs, as the initial  $[N-j-1]$  and final  $[N-j]$  eigenstates of the negative temperature discrete ESTs are offset by one quantum of energy from the initial  $[N-j]$  and final  $[N-j+1]$  eigenstates of the negative temperature continuous ESTs.

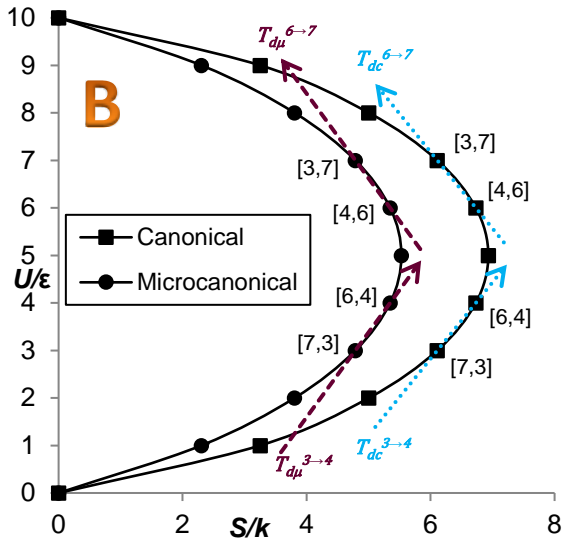
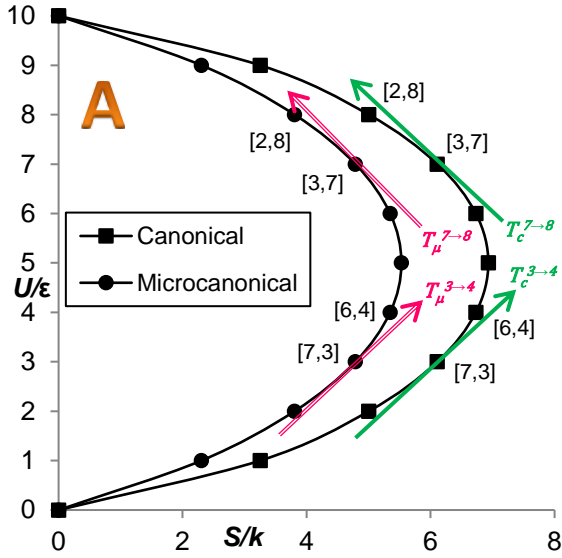
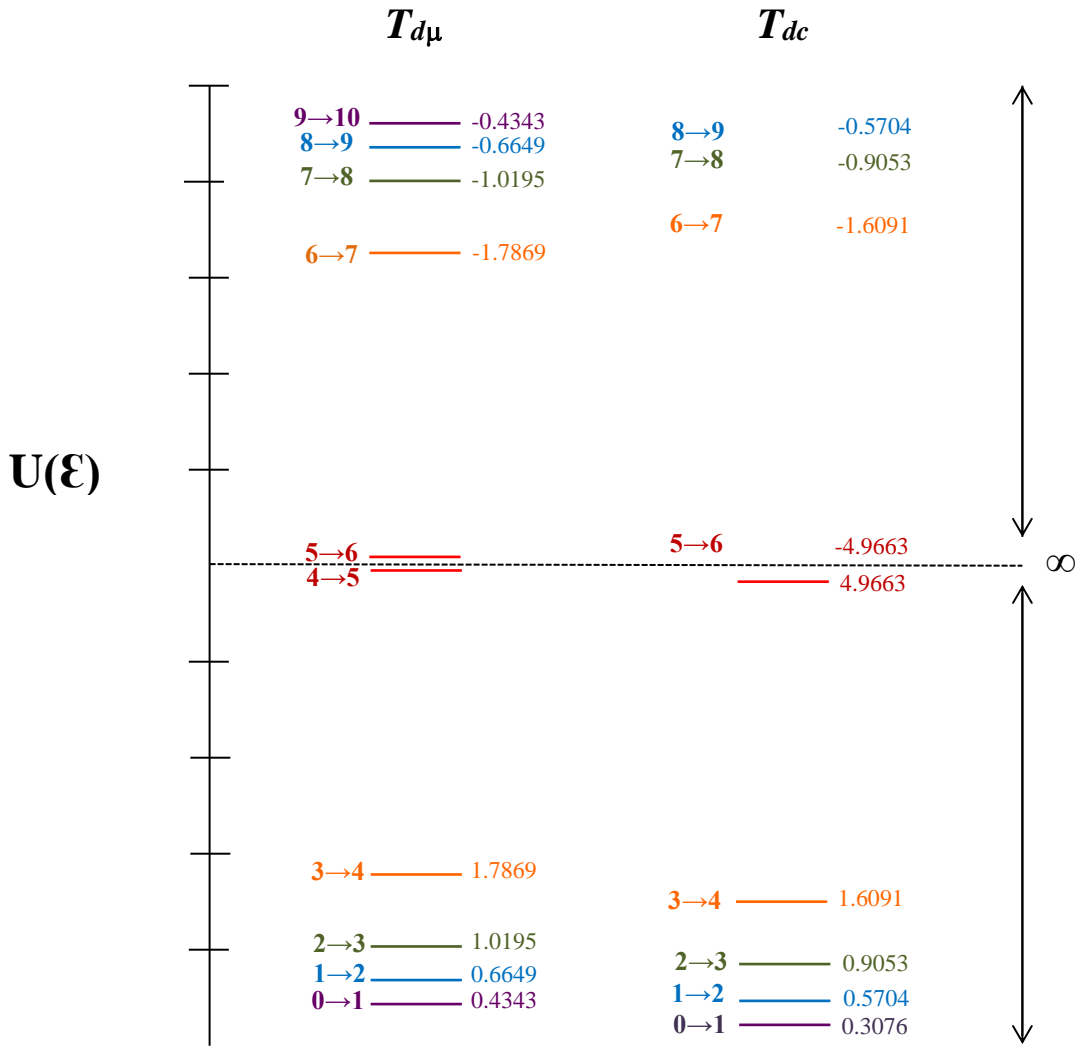


**Fig. A-1.** (A) Continuous microcanonical (red) and canonical (green) spin permutation antisymmetries  $T^{7 \rightarrow 8} = -T^{3 \rightarrow 4}$  for two-level PSLs (see Eqs. A1a,A1b and Fig. A-2B). (B) Discrete microcanonical (brown dashed) and canonical (blue dotted) spin permutation antisymmetries  $T^{6 \rightarrow 7} = -T^{3 \rightarrow 4}$  for two-level PSLs (see Eqs. A2a,A2b and Fig. A-2A).

## A. Discrete SPAs



## B. Continuous SPAs

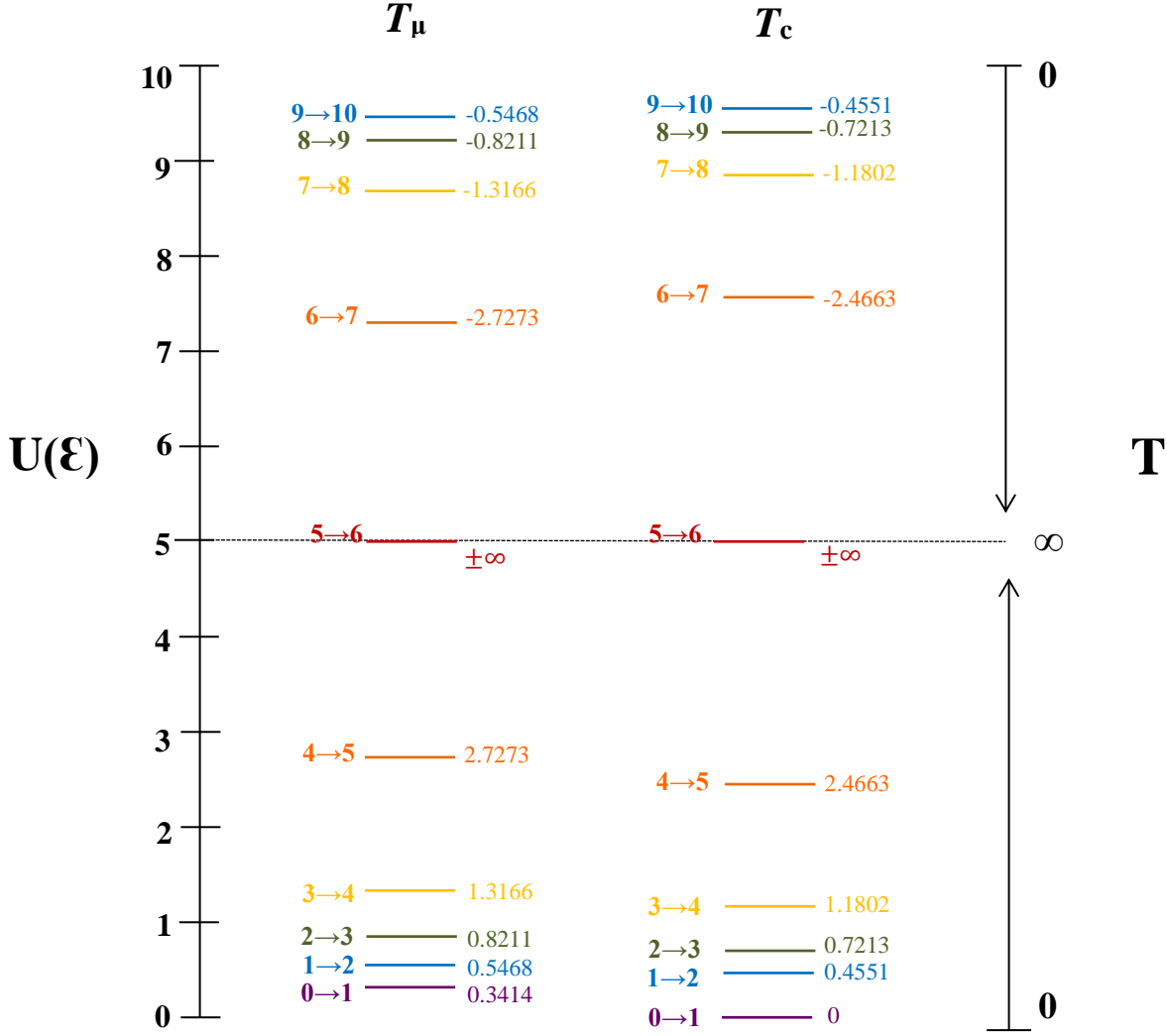


**Fig. A-2.** (A) *Discrete* spin permutation antisymmetries  $T_{dc}^{N-j-1 \rightarrow N-j} = -T_{dc}^{j \rightarrow j+1}$  and  $T_{d\mu}^{N-j-1 \rightarrow N-j} = -T_{d\mu}^{j \rightarrow j+1}$  and (B) *continuous* spin permutation antisymmetries  $T_c^{N-j \rightarrow N-j+1} = -T_c^{j \rightarrow j+1}$  and  $T_\mu^{N-j \rightarrow N-j+1} = -T_\mu^{j \rightarrow j+1}$  for an  $N = 10$  PSL.

## APPENDIX B

### SYSTEM SIZE-DEPENDENCE OF CONSTANT- $X_j$ , DECREASING- $X_j$ , AND INCREASING- $X_j$

#### EIGENSTATES IN TWO-LEVEL PSLs

The eigenstates of PSLs fall into three basic categories: *Constant- $X_j$* , *Decreasing- $X_j$* , and *Increasing- $X_j$*  (see Eqs. [14a,b,c], Secs. III.C, and Figs. 3,4). This terminology specifies the behavior of the spin-down mole fraction

$$X_j = \frac{N_\downarrow}{N} = \frac{j}{N}, \quad (\text{B1})$$

which either remains constant, decreases, or increases with increasing  $N$  depending on the mathematical form of the spin-down quantum number  $j$  and the spin-down mole fraction  $X_j$  of the initial eigenstates in  $\Delta j = +1$  transitions:

$$j = aN = X_j N; \quad X_j = a \quad (\text{for Constant-}X_j \text{ eigenstates}),^1 \quad (\text{B2a})$$

$$j = aN - 1 = X_j N; \quad X_j = a - \frac{1}{N} \quad (\text{for Increasing-}X_j \text{ eigenstates}),^2 \quad (\text{B2b})$$

and

$$j = aN + 1 = X_j N; \quad X_j = a + \frac{1}{N} \quad (\text{for Decreasing-}X_j \text{ eigenstates}),^3 \quad (\text{B2c})$$

in which the constant  $0 < a \leq 1$ . The  $N$ -dependence of these three categories of eigenstates are detailed below.

#### 1. ESTs of Constant- $X_j$ Eigenstates

---

<sup>1</sup> E.g.,  $a = 0.25$  for the  $[0.75N, 0.25N] \rightarrow [(0.75N-1), (0.25N+1)]$ ,  $\Delta j = +1$  transition originating from the  $j = 0.25N$ ,  $X_j = 0.25$  eigenstate, etc.

<sup>2</sup> E.g.,  $a = 0.25 - 1/N$  for the  $[(0.75N+1), (0.25N-1)] \rightarrow [(0.75N), (0.25N)]$ ,  $\Delta j = +1$  transition originating from the  $j = 0.25N - 1$ ,  $X_j = 0.25 - 1/N$  eigenstate, etc.

<sup>3</sup> E.g.,  $a = 0.25 + 1/N$  for the  $[(0.75N-1), (0.25N+1)] \rightarrow [(0.75N-2), (0.25N+2)]$ ,  $\Delta j = +1$  transition originating from the  $j = 0.25N + 1$ ,  $X_j = 0.25 + 1/N$  eigenstate, etc.

The ESTs of Constant- $X_j$  eigenstates  $[(1-a)N, aN]$  are obtained by combining Eq. (B1) with Eqs. (8a,b,10,12,13) to yield

$$T_{\mu}^{X_j \rightarrow X_j + \frac{1}{N}} = T_{\mu}^{aN \rightarrow aN+1} = \frac{\varepsilon}{k(\Psi_0[(1-a)N+1] - \Psi_0[aN+1])} = \frac{\varepsilon}{k\left(\sum_{p=1}^{(1-a)N} \frac{1}{p} - \sum_{p=1}^{aN} \frac{1}{p}\right)}, \quad (\text{B3})$$

$$T_c^{X_j \rightarrow X_j + \frac{1}{N}} = T_c^{aN \rightarrow aN+1} = \frac{\varepsilon}{k \ln\left(\frac{1-a}{a}\right)}, \quad (\text{B4})$$

$$T_{d\mu}^{X_j \rightarrow X_j + \frac{1}{N}} = T_{d\mu}^{aN \rightarrow aN+1} = \frac{\varepsilon}{k \ln\left(\frac{(1-a)N}{aN+1}\right)}, \quad (\text{B5})$$

and

$$T_{\mu}^{X_j \rightarrow X_j + \frac{1}{N}} = T_{dc}^{aN \rightarrow aN+1} = \frac{\varepsilon}{kN(1-a) \ln\left[\frac{(1-a)N}{(1-a)N-1}\right] + akN \ln\left(\frac{aN}{aN+1}\right) + k \ln\left[\frac{(1-a)N-1}{aN+1}\right]}, \quad (\text{B6})$$

$T_{\mu}^{X_j \rightarrow X_j + \frac{1}{N}}$ ,  $T_{d\mu}^{X_j \rightarrow X_j + \frac{1}{N}}$ , and  $T_{dc}^{X_j \rightarrow X_j + \frac{1}{N}}$  are all larger than the thermodynamic-limiting value<sup>6</sup>  $\varepsilon/k \ln[(1-a)/a]$  at small  $N$ , but descend to  $\varepsilon/k \ln[(1-a)/a]$  in the TDL (see Sec. III.C; Fig. 3a,c,d); *i.e.*, the continuous microcanonical, discrete microcanonical and discrete canonical ESTs of Constant- $X_j$  eigenstates are thus non-intensive at small  $N$ , but become intensive in the TDL.<sup>6</sup> In contrast,  $T_c^{X_j \rightarrow X_j + \frac{1}{N}}$  is equal to the thermodynamic-limiting value for all  $N$ ; *i.e.*, the continuous canonical ESTs of all Constant- $X_j$  eigenstates are inherently intensive. For example, the ESTs



$T_{\mu}^{\frac{N}{4} \rightarrow \frac{N}{4} + 1}$ ,  $T_{d\mu}^{\frac{N}{4} \rightarrow \frac{N}{4} + 1}$  and  $T_{dc}^{\frac{N}{4} \rightarrow \frac{N}{4} + 1}$  are all larger than  $\varepsilon/k\ln[(1-a)/a] = \varepsilon/k\ln 3$  at small  $N$ , and converge

to  $\varepsilon/k\ln 3$  at large  $N$ , whereas  $T_c^{\frac{N}{4} \rightarrow \frac{N}{4} + 1}$  is equal to  $\varepsilon/k\ln 3$  for all  $N$ .

## 2. ESTs of Increasing- $X_j$ Eigenstates

The ESTs of Increasing- $X_j$  eigenstates  $[(1-a)N + 1, (aN - 1)]$  are obtained by combining Eq. (B1) with Eqs. (8a,b,10,12,13) to yield

$$T_{\mu}^{X_j \rightarrow X_j + \frac{1}{N}} = T_{\mu}^{aN-1 \rightarrow aN} = \frac{\varepsilon}{k(\Psi_0[(1-a)N + 2] - \Psi_0[aN])} = \frac{\varepsilon}{k\left(\sum_{p=1}^{(1-a)N+1} \frac{1}{p} - \sum_{p=1}^{aN-1} \frac{1}{p}\right)}, \quad (\text{B7})$$

$$T_c^{X_j \rightarrow X_j + \frac{1}{N}} = T_c^{aN-1 \rightarrow aN} = \frac{\varepsilon}{k\ln\left(\frac{(1-a)N + 1}{aN - 1}\right)}, \quad (\text{B8})$$

$$T_{d\mu}^{X_j \rightarrow X_j + \frac{1}{N}} = T_{d\mu}^{aN-1 \rightarrow aN} = \frac{\varepsilon}{k\ln\left(\frac{(1-a)N + 1}{aN}\right)}, \quad (\text{B9})$$

and

$$T_{dc}^{X_j \rightarrow X_j + \frac{1}{N}} = T_{dc}^{aN-1 \rightarrow aN} = \frac{\varepsilon}{k[(1-a)N - 1]\ln\left[\frac{(1-a)N - 1}{(1-a)N - 2}\right] + k(aN - 1)\ln\left(\frac{aN - 1}{aN}\right) + k\ln\left[\frac{(1-a)N - 2}{aN}\right]}. \quad (\text{B10})$$

These four expressions are all smaller than the thermodynamic-limiting value<sup>6</sup>  $\varepsilon/k\ln[(1-a)/a]$  at small  $N$ , but ascend to  $\varepsilon/k\ln[(1-a)/a]$  in the TDL (see Sec. III.C; Fig. 4a):

$$\lim_{N \rightarrow \infty} T_{\mu}^{aN-1 \rightarrow aN} = \lim_{N \rightarrow \infty} T_c^{aN-1 \rightarrow aN} = \lim_{N \rightarrow \infty} T_{d\mu}^{aN-1 \rightarrow aN} = \lim_{N \rightarrow \infty} T_{dc}^{aN-1 \rightarrow aN}$$

$$= \frac{\varepsilon}{k \ln \left( \frac{1-a}{a} \right)} = \frac{\varepsilon}{k \ln \left( \frac{1-X_j}{X_j} \right)} \quad (\text{B11})$$

For example, all four ESTs originating from the  $j = 0.25N - 1$ ,  $X_j = 0.25 - 1/N$  ESTs are smaller than  $\varepsilon/k \ln[(1-a)/a] = \varepsilon/k \ln 3$  at small  $N$ , and converge to  $\varepsilon/k \ln 3$  at large  $N$ .

### 3. ESTs of Decreasing- $X_j$ Eigenstates

The ESTs of Decreasing- $X_j$  eigenstates [ $\{(1-a)N-1\}$ ,  $(aN+1)$ ] are obtained by combining Eq. (B1) with Eqs. (8a,b,10,12,13) to yield

$$T_{\mu}^{X_j \rightarrow X_j + \frac{1}{N}} = T_{\mu}^{aN+1 \rightarrow aN+2} = \frac{\varepsilon}{k \left( \Psi_0[(1-a)N] - \Psi_0[aN+2] \right)} = \frac{\varepsilon}{k \left( \sum_{p=1}^{(1-a)N-1} \frac{1}{p} - \sum_{p=1}^{aN+1} \frac{1}{p} \right)}, \quad (\text{B12})$$

$$T_c^{X_j \rightarrow X_j + \frac{1}{N}} = T_c^{aN+1 \rightarrow aN+2} = \frac{\varepsilon}{k \ln \left( \frac{[1-a]N-1}{aN+1} \right)}, \quad (\text{B13})$$

$$T_{d\mu}^{X_j \rightarrow X_j + \frac{1}{N}} = T_{d\mu}^{aN+1 \rightarrow aN+2} = \frac{\varepsilon}{k \ln \left( \frac{[1-a]N-1}{aN+2} \right)}, \quad (\text{B14})$$

$$T_{dc}^{X_j \rightarrow X_j + \frac{1}{N}} = T_{dc}^{aN+1 \rightarrow aN+2} = \frac{\varepsilon}{k[(1-a)N+1] \ln \left[ \frac{(1-a)N+1}{(1-a)N} \right] + k(aN+1) \ln \left( \frac{aN+1}{aN+2} \right) + k \ln \left[ \frac{(1-a)N}{aN+2} \right]}. \quad (\text{B15})$$

These four expressions all larger than the thermodynamic-limiting value<sup>6</sup>  $\varepsilon/k \ln[(1-a)/a]$  at small  $N$ , but descend to  $\varepsilon/k \ln[(1-a)/a]$  in the TDL (see Sec. III.C; Fig. 4b,c):

$$\lim_{N \rightarrow \infty} T_{\mu}^{aN+1 \rightarrow aN+2} = \lim_{N \rightarrow \infty} T_c^{aN+1 \rightarrow aN+2} = \lim_{N \rightarrow \infty} T_{d\mu}^{aN+1 \rightarrow aN+2} = \lim_{N \rightarrow \infty} T_{dc}^{aN+1 \rightarrow aN+2}$$

$$= \frac{\varepsilon}{k \ln \left( \frac{1-a}{a} \right)} = \frac{\varepsilon}{k \ln \left( \frac{1-X_j}{X_j} \right)} . \quad (\text{A16})$$

For example, all four ESTs originating from the  $j = 0.25N - 1$ ,  $X_j = 0.25 + 1/N$  eigenstates are larger than  $\varepsilon/k \ln[(1-a)/a] = \varepsilon/k \ln 3$  at small  $N$ , and converge to  $\varepsilon/k \ln 3$  at large  $N$ .

In summary, the continuous canonical ESTs of Constant- $X_j$  eigenstates are equal to the common thermodynamic-limiting value  $\varepsilon/k \ln[(1-a)/a]$  for *all*  $N$  and are thus *inherently intensive*. In contrast, all four ESTs of Decreasing- $X_j$  eigenstates and Increasing- $X_j$  eigenstates, as well as the continuous microcanonical, discrete microcanonical and discrete canonical ESTs of Constant- $X_j$  eigenstates all *converge to* the thermodynamic-limiting value at large  $N$ ; these ESTs are inherently non-intensive at finite  $N$ , but become intensive in the TDL.<sup>6,7</sup>

## REFERENCES

<sup>1</sup>de Miguel and Rubi obtain a different—but related—set of spin permutation antisymmetries for the discrete microcanonical ESTs  $T_{d\mu}^{j-1 \rightarrow j}$  defined in terms of "backward"  $j-1 \rightarrow j$  transitions. Our four ESTs are all defined in terms of "forward"  $j \rightarrow j+1$  transitions ("forward" and "backward" terminology taken from Ref. 33 and from T. Wada and A.M. Scarfone, J. Phys. Conf. Ser. **201**, 0125 [2010]).

<sup>2</sup>Using backward  $j = -1 \rightarrow j = 0$  transitions (see Refs. 33, 119), de Miguel and Rubi find that the discrete microcanonical temperature of the perfect crystalline (*i.e.*, all–spins–down) PSL ground state  $[N, 0]$  is equal to zero:  $T_{d\mu}^{j-1 \rightarrow j} = T_{d\mu}^{-1 \rightarrow 0} = 0$ , in accord with the Third Law. However, to obtain this result, they must assume that the ground state temperature is equal to that of a transition originating from a non–physical  $[N+1, -1]$  "eigenstate" lying below the ground eigenstate. In contrast, we assume that the ground state temperature  $T_{d\mu}^{j \rightarrow j+1} = T_{d\mu}^{0 \rightarrow 1}$  is equal to that of a forward  $j = 0 \rightarrow j = 1$  transition between the two genuine, physical PSL eigenstates  $[N, 0]$  and  $[N-1, 1]$ . While the forward continuous canonical EST  $T_c^{0 \rightarrow 1}$  is equal to zero for all  $N$ , the forward ESTs  $T_{d\mu}^{0 \rightarrow 1}$ ,  $T_\mu^{0 \rightarrow 1}$  and  $T_{dc}^{0 \rightarrow 1}$  are all greater than zero for finite  $N$  and approach zero in the limit of large  $N$ . Our results thus indicate that for the ground state in PSLs, forward ESTs are consistent with the Third Law—but generally only in the TDL.

It is interesting to note that for  $j = N \rightarrow j = N+1$  transitions from the perfect crystalline (*i.e.* all–spins–down), maximum energy eigenstate  $[0, N]$  to the non–physical state  $[-1, N+1]$  directly above it, backward  $T_{d\mu}^{j-1 \rightarrow j}$  values are finite and negative and approach  $-0$  in the thermodynamic limit, whereas forward  $T_{d\mu}^{j \rightarrow j+1}$  values are equal to  $-0$  for all  $N$ ; *i.e.*, there is a symmetry between the  $N$ –dependence of  $T_{d\mu}^{j-1 \rightarrow j}$  and  $T_{d\mu}^{j \rightarrow j+1}$  for the  $[N, 0]$  and  $[0, N]$  eigenstates, which suggests a difference in zero–point energy for backward and forward discrete microcanonical ESTs. This symmetry is related to the spin permutation antisymmetries and may be rooted in the differences in the Second Law for negative and positive temperature eigenstates proposed by Lavenda (see Sec. III.B, the supporting materials, and Ref. 8).

<sup>3</sup>The presence of the functional  $X_j$ –dependencies in both forward and backward discrete microcanonical ESTs (see Refs. 33, 119) precludes the possibility that these  $X_j$ –dependencies originate from temperature–dependent system energy levels (TDSELs), since the Hamiltonians of thermally–isolated systems are not perturbed by bath Hamiltonians.

<sup>4</sup> $[N+1, -1] \rightarrow [N, 0]$  and  $[0, N] \rightarrow [-1, N+1]$  transitions are not *physically* realistic because  $[N+1, -1]$  and  $[-1, N+1]$  are not PSL eigenstates. These transitions are accordingly not discussed in the text, though  $T_c^{conv}$ ,  $T_c^{j \rightarrow j+1}$ ,  $T_\mu^{j \rightarrow j+1}$  and  $T_{dc}^{j \rightarrow j+1}$  are *mathematically* well–behaved for  $j = -1$  and  $N$ , as is  $T_{d\mu}^{j \rightarrow j+1}$  for  $j = N$ .

<sup>5</sup>Eqs. (B5,9,14) are expanded versions of Eq. (12) which facilitate the elucidation of the thermodynamic–limiting values of the discrete microcanonical temperature of constant– $X_j$ , increasing– $X_j$ , and decreasing– $X_j$  ESTs.

<sup>6</sup>The continuous canonical ESTs of all Increasing– $X_j$  and Decreasing– $X_j$  eigenstates are equal to the thermodynamic–limiting value  $\varepsilon/k\ln[(1-a)/a] = \varepsilon/k\ln[(1-X_j)/X_j]$  for all  $N$  and are thus inherently intensive. The continuous microcanonical from–the–vertex EST is likewise equal to  $\varepsilon/k\ln[(1-a)/a] = \varepsilon/k\ln[(1-X_j)/X_j]$  for all  $N$  in the limit as  $j \rightarrow (N/2)^\pm$  and is inherently intensive; it is unique among continuous microcanonical ESTs in this regard. The ESTs of Increasing– $X_j$

and Decreasing- $X_j$  eigenstates converge only in the TDL, and are thus non-intensive (see Sec. III.C).

<sup>7</sup>The  $X_j$ -dependence of our forward ( $T_{dt}^{j \rightarrow j+1}$ ) and de Miguel and Rubi's backward ( $T_{dt}^{j-1 \rightarrow j}$ ) discrete microcanonical ESTs (see Refs. 33 and 119) are opposite to each other. For example, the values of  $T_{dt}^{j \rightarrow j+1}$  are large for small  $N$  and fall to their thermodynamic limiting values near  $N = 1,000$  (see Fig. 3c in the revised manuscript), whereas the values of  $T_{dt}^{j-1 \rightarrow j}$  are small for small  $N$  and rise to their intensive, thermodynamic limiting values near  $N = 1,000$  (from our plots of de Miguel and Rubi's  $T_{dt}^{j-1 \rightarrow j}$  values; data not shown).